AMERICAN SOCIETY FOR MICROBIOLOGY | Journal of Virology

A Novel Live Pichinde Virus-Based Vaccine Vector Induces Enhanced Humoral and Cellular Immunity after a Booster Dose

Rekha Dhanwani,[a]* Yanqin Zhou,[a,b] Qinfeng Huang,[a,c] Vikram Verma,[a] Mythili Dileepan,[a] Hinh Ly,[a] Yuying Liang[a]

Department of Veterinary and Biomedical Sciences, College of Veterinary Medicine, University of Minnesota, Twin Cities, Minnesota, USA[a]; College of Veterinary Medicine, Huazhong Agricultural University, Wuhan, Hubei, China[b]; Department of Swine Infectious Diseases, Shanghai Veterinary Research Institute, Chinese Academy of Agricultural Sciences, Shanghai, China[c]

ABSTRACT

Pichinde virus (PICV) is a bisegmented enveloped RNA virus that targets macrophages and dendritic cells (DCs) early in infection and induces strong innate and adaptive immunity in mice. We have developed a reverse genetics system to produce live recombinant PICV (strain P18) with a trisegmented RNA genome (rP18tri), which encodes all four PICV gene products and as many as two foreign genes. We have engineered the vector to express the green fluorescent protein (GFP) reporter gene (abbreviated as G in virus designations) and either the hemagglutination (HA [H]) or the nucleoprotein (NP [P]) gene of the influenza A/PR8 virus. The trisegmented viruses rP18tri-G/H and rP18tri-G/P showed slightly reduced growth *in vitro* and expressed HA and NP, respectively. Mice immunized with rP18tri-G/H were completely protected against lethal influenza virus challenge even 120 days after immunization. These rP18tri-based vectors could efficiently induce both neutralizing antibodies and antigen-specific T cell responses via different immunization routes. Interestingly, the immune responses were significantly increased upon a booster dose and remained at high levels even after three booster doses. In summary, we have developed a novel PICV-based live vaccine vector that can express foreign antigens to induce strong humoral and cell-mediated immunity and is ideal for a prime-and-boost vaccination strategy.

IMPORTANCE

We have developed a novel Pichinde virus (PICV)-based live viral vector, rP18tri, that packages three RNA segments and encodes as many as two foreign genes. Using the influenza virus HA and NP genes as model antigens, we show that this rP18tri vector can induce strong humoral and cellular immunity via different immunization routes and can lead to protection in mice. Interestingly, a booster dose further enhances the immune responses, a feature that distinguishes this from other known live viral vectors. In summary, our study demonstrates a unique feature of this live rP18tri vector to be used as a novel vaccine platform for a prime-and-boost vaccination strategy.

Arenaviruses are enveloped RNA viruses with a bisegmented genome and mostly use rodents as natural hosts. There are at least 27 members that are geographically, serologically, and phylogenetically divided into Old World and New World arenaviruses (1). The prototypic lymphocytic choriomeningitis virus (LCMV) infection of mice has long been used as a valuable model with which to study viral persistence and virus-induced immunity and immunopathology (2, 3). The arenavirus is composed of a total of four genes on two genomic RNA segments in opposite orientations (1). The Z protein, produced from the large (L) genomic segment, is a small RING domain-containing matrix protein that mediates virus budding, regulates viral RNA synthesis, and mediates host immune suppression (4, 5). The large L protein (~200 kDa), also encoded on the L segment, is the RNA-dependent RNA polymerase (RdRp), which is required for viral RNA synthesis (6). The glycoprotein (GPC), encoded on the small (S) segment, is posttranslationally processed into a stable signal peptide (SSP), the receptor-binding G1 protein, and the transmembrane G2 protein (7). The nucleoprotein (NP) of the S segment encapsidates viral genomic RNAs and is required for viral RNA synthesis and host immune suppression (8–13).

Arenaviruses are known to target dendritic cells (DCs) and macrophages early in infection and have been explored as potential vaccine vectors. An LCMV-based replication-defective vaccine vector in which the viral GPC gene is replaced by the ovalbumin (OVA) antigen has been developed. This vector can propagate in cells engineered to constitutively express GPC and can elicit strong cytotoxic T-lymphocyte (CTL) responses in mice (14). In order to generate a replication-competent virus to deliver genes of interest, Emonet and colleagues have developed a trisegmented system for LCMV that can encode as many as two foreign genes (15, 16). A similar recombinant trisegmented system has also been developed for the Junin arenavirus vaccine strain (Candid#1) and has been propagated in the Food and Drug Administration (FDA)-approved Vero cell line (17).

Pichinde virus (PICV) is an arenavirus isolated from rice rats

Received 20 October 2015 **Accepted** 11 December 2015

Accepted manuscript posted online 16 December 2015

Citation Dhanwani R, Zhou Y, Huang Q, Verma V, Dileepan M, Ly H, Liang Y. 2016. A novel live Pichinde virus-based vaccine vector induces enhanced humoral and cellular immunity after a booster dose. J Virol 90:2551–2560. doi:10.1128/JVI.02705-15.

Editor: D. S. Lyles

Address correspondence to Yuying Liang, liangy@umn.edu.

* Present address: Rekha Dhanwani, La Jolla Institute for Allergy and Immunology, La Jolla, California, USA.

H.L. and Y.L. are co-senior authors.

(*Oryzomys albigularis*) in Columbia (reviewed in reference 18). Serological evidence suggests a very low seroprevalence: even in the local human population, only 2 out of 82 people tested in the habitats of infected rodents have shown evidence of seroconversion (19). Since PICV is geographically restricted by its natural host, there is little to no preexisting immunity against PICV in the general human population, in contrast to LCMV, which has 2 to 5% seroprevalence in human populations (20). In general, PICV is not known to cause diseases in humans. There is evidence that PICV can cause asymptomatic human infections in a laboratory setting, in which 6 out of 13 (46%) persons working with the virus showed positive sera but no distinct illness (21). The generally innocuous nature of PICV is also supported by our recent molecular analysis of the viral gene products. We found that the Z proteins of all known human arenavirus pathogens, including the low-risk pathogen LCMV and the highly virulent pathogen Lassa fever virus (LASV), but not those of others such as PICV, can inhibit the RIG-I-like receptors (RLRs) (5). Therefore, we believe that PICV has a better biosafety profile than LCMV, but like LCMV, PICV can induce strong immune responses, especially cellular immunity (19, 22). Mice infected with high doses of PICV (up to 4×10^7 PFU) through the intraperitoneal (i.p.), intracranial (i.c.), or intravenous (i.v.) inoculation route can clear the virus quickly (by 4 days postinfection [dpi]) without any disease signs, due to the activated spleen natural killer (NK) cell activity, followed by the virus-specific CTL responses (19, 22). We have previously developed a reverse genetics system to generate infectious PICV from two plasmids that produce full-length antigenomic strands of the L and S RNAs (23). Using this reverse genetics system, we have characterized the functional mechanisms of viral virulence determinants and the biological roles of arenaviral proteins (13, 24–28).

We report here the development of a trisegmented recombinant PICV (strain P18) (rP18tri) system as a novel vaccine vector. Using the rP18tri vectors expressing influenza virus antigens (hemagglutinin [HA] and/or NP), we show that these viral vectors can induce protective immunity against a lethal influenza virus challenge in mice. Unexpectedly, instead of seeing waning levels of vaccine immunity after repeated applications, we have observed enhanced vaccine-specific humoral and cellular immune responses after a booster dose, a unique feature that is ideal for use in the prime-boost vaccination regimen.

MATERIALS AND METHODS

Cells and viruses. BHK-21 baby hamster kidney cells, Vero African green monkey kidney cells, and Madin-Darby canine kidney (MDCK) cells were maintained in Dulbecco's modified Eagle medium (DMEM) supplemented with 10% fetal bovine serum (FBS) and 50 μg/ml penicillin-streptomycin. BSRT7-5 cells, which are BHK-21 cells stably expressing T7 RNA polymerase, were obtained from K.-K. Conzelmann (Ludwig-Maximilians-Universität, Munich, Germany) and were cultured in minimal essential medium (MEM) (Invitrogen-Life Technologies) supplemented with 10% FBS, 1 μg/ml Geneticin (Invitrogen-Life Technologies), and 50 μg/ml penicillin-streptomycin. Recombinant PICVs were plaque purified and were amplified in BHK-21 cells, and the infectious virus titer was determined by a plaque assay in Vero cells as described previously (23). Mouse-adapted A/PR8 influenza viruses were grown in embryonic eggs; viral titers were quantified by plaque assays on MDCK cells, and lethal dosages in mice were determined.

Plasmids. The plasmids expressing the full-length antigenomic strands of the PICV L and S segments from the T7 promoter, pUC18-P18Lag and pUC18-P18Sag, have been described previously (23). The overlapping PCR method was used to replace the GPC and NP open reading frames (ORFs) on the pUC18-P18Sag vector with multiple cloning sites (MCS), generating P18S-GPC/MCS (the S1 plasmid) and P18S-MCS/NP (the S2 plasmid), respectively. The enhanced green fluorescent protein (eGFP) reporter gene was amplified by PCR and was subcloned into the S2 plasmid between the NheI and KpnI sites to generate the P18S-GFP/NP plasmid. The HA and NP genes of influenza virus A/PR8 were amplified from plasmids expressing full-length influenza virus A/PR/8 HA and NP and were subcloned into the S1 plasmid between the NheI and XhoI sites to generate the P18S-GPC/PR8HA and P18S-GPC/PR8NP plasmids, respectively.

Rescue of recombinant trisegmented Pichinde viruses (rP18tri) from plasmids by transfection. Recombinant viruses were recovered from plasmids by transfecting BSRT7-5 (also called BHK-T7) cells with 3 plasmids: pUC18-P18Lag, P18S-GPC/PR8HA or P18S-GPC/PR8NP, and P18S-GFP/NP (see Fig. 2B). The procedures used to generate recombinant PICV are essentially the same as those described previously (23). Briefly, BHK-T7 cells were grown overnight to 80% confluence, and 4 h before transfection, the cells were washed and were incubated with antibiotic-free DMEM (Sigma-Aldrich). For transfection, 2 μg of each plasmid was diluted in 250 μl of Opti-MEM (Invitrogen-Life Technologies) and was incubated at room temperature for 15 min. An equal volume of Opti-MEM with 10 μl of Lipofectamine (Invitrogen-Life Technologies) was added, and the mixture was incubated for 20 min at room temperature. Following incubation, the cells were transfected with the plasmids, and a fresh aliquot of DMEM was added after 4 h to remove the Lipofectamine. After 48 h of transfection, cell supernatants were collected for a plaque assay. Virus grown from individual plaques was used to prepare stocks that were grown on BHK-21 cells and were stored at −80°C.

Detection of influenza virus antigen expression in cells infected with recombinant trisegmented PICV vaccine vectors. BHK-21 cells grown on coverslips were infected at a multiplicity of infection (MOI) of 1 with the rP18tri vectors expressing GFP and the influenza virus HA or NP gene. At 24 h postinfection (hpi), the cells were fixed with 4% paraformaldehyde for 15 min at room temperature, followed by three washes with phosphate-buffered saline (PBS) (Invitrogen-Life Technologies). The cells were then incubated in 0.1% Triton X-100 for 12 min, followed by a 1-h incubation with the primary antibody (polyclonal mouse anti-H1N1 serum for HA and mouse anti-influenza virus A nucleoprotein antibody for NP) (AbD Serotec, Raleigh, NC). The cells were then washed and incubated with a secondary antibody (an Alexa Fluor 594-labeled goat anti-mouse antibody) (Invitrogen) for 1 h at room temperature. After three washes, the cells on coverslips were mounted on glass slides and were observed under a fluorescence microscope.

Guinea pig infection and immunization. The experimental procedures for guinea pigs followed the approved protocol of the Institutional Animal Care and Use Committee (IACUC) of the University of Minnesota. Male Hartley guinea pigs weighing 200 to 250 g were acclimatized for 3 days in the institutional animal facility. For virulence determination, guinea pigs were injected intraperitoneally with 10,000 PFU of recombinant PICV (strain P18) (rP18) or trisegmented rP18tri vector expressing GFP (rP18tri-G), or with PBS for mock infection. Rectal temperature and body weight were measured daily up to 18 days. Fever was defined as a rectal temperature of >39.5°C. Guinea pigs were declared moribund and were euthanized if their body weight decreased 30% from that of the control group. For immunization purposes, guinea pigs were infected intraperitoneally with 10,000 PFU of rP18tri-G or trisegmented rP18tri vector expressing GFP and the influenza A virus HA gene (rP18tri-G/H). Blood was drawn at days 14 and 28 for hemagglutination inhibition (HAI) analysis.

Mouse immunization and challenge. The experimental procedures for mice followed the approved protocol of the IACUC of the University of Minnesota. Six- to 8-week-old female C57BL/6 mice were obtained from Charles River Laboratories and were housed for at least 1 week for

acclimatization. Mice were immunized with 1,000 to 100,000 PFU of rP18tri-based viral vaccine vectors through various routes: intraperitoneal (i.p.), intramuscular (i.m.), and intranasal (i.n.). Relatively low numbers of animals (*n*, 3 or 5) were used in some of these experiments in order to provide a quick assessment of the optimal parameters for subsequent experiments with larger numbers of animals. Boosting with the same vaccine vector was performed at a 14-day interval. Fourteen days after the last vaccination dose (unless otherwise specified for the longer protection study), mice were challenged intranasally with 10 MLD_{50} (50% minimal lethal doses) of the mouse-adapted influenza A/PR8 virus strain and were monitored for body weight and disease symptoms for as long as 14 days. Blood was collected at different time points during the vaccination and/or challenge period for immunological analyses. Lungs were collected at 6 days postchallenge for viral titer quantification by plaque assays, for pathological analysis by hematoxylin-and-eosin (H&E) staining, and for viral antigen detection by immunohistochemical (IHC) staining with an anti-NP antibody.

Analysis of NP-specific CTL responses by tetramer staining. The phycoerythrin (PE)-labeled H-$2D^b$ tetramer with the influenza virus $NP_{366-374}$ epitope ASNENMETM was previously provided by the NIH Tetramer Core Facility at Emory University (Atlanta, GA) and was later obtained from MBL International (Woburn, MA). Single-cell splenocytes were obtained, and red blood cells (RBCs) were lysed using ACK (ammonium-chloride-potassium) lysis buffer (eBioscience). The splenocytes were then washed twice with fluorescence-activated cell sorting (FACS) buffer (PBS plus 2% FBS). A total of 1×10^5 cells were stained with peridinin chlorophyll protein (PerCP)-Cy5.5-labeled CD8, allophycocyanin (APC)-labeled CD3, fluorescein isothiocyanate (FITC)-labeled CD4, and the PE-labeled H-$2D^b$ tetramer with the $NP_{366-374}$ epitope ASNEN METM for 1 h at room temperature. After incubation, cells were washed three times with FACS buffer, and the labeled cells were analyzed with a FACSCanto instrument (BD Biosciences, San Jose, CA, USA). The FACS data were analyzed using FlowJo software (Tree Star, Ashland, OR).

Hemagglutination inhibition assay. Blood was collected from the animals 14 days after each immunization, and serum was harvested from the blood. Nonspecific inhibitors were removed from the serum by overnight treatment with 5 volumes of receptor-destroying enzyme (Sigma-Aldrich), followed by 45 min of incubation at 56°C to inactivate the enzyme and the serum. Each serum sample was serially diluted in 25 μl of PBS and was then mixed with an equal volume of PBS containing 4 HA units of the mouse-adapted influenza A/PR8 virus. After 15 min of incubation at room temperature, 50 μl of 0.5% turkey RBCs was added, and the mixture was incubated for 1 h at 4°C before the evaluation of agglutination. The titer was recorded as the inverse of the last dilution that inhibited agglutination.

RESULTS

Generation of recombinant trisegmented PICV (rP18tri) expressing GFP. We previously developed a two-plasmid-based reverse genetics system to generate an authentic recombinant Pichinde virus with a bisegmented RNA genome (23) (Fig. 1A, top). To generate a trisegmented recombinant PICV (strain P18), we modified the S RNA-encoding plasmid by replacing the NP or GPC gene with multiple cloning sites (MCS) to generate the S1 and S2 vectors, respectively, and subsequently engineered the GFP reporter gene into the MCS of the S2 vector. All three plasmids (the L, S1, and S2 plasmids) were transfected into BHK-T7 cells, from which infectious viral particles (rP18tri-G) would contain all three RNA segments (L, S1, and S2) (Fig. 1A, bottom). Supernatants from the transfected cells were collected and were analyzed by plaque assays on Vero cells. As expected, both the plasmid-transfected BHK-T7 cells and the supernatant-infected Vero cells expressed GFP, as observed under fluorescence microscopy (Fig. 1B, bottom left), in contrast to cells infected with the non-GFP-encoding parental rP18 virus (Fig. 1B, top left). The rP18tri-G virus forms smaller plaques than the parental rP18 virus (Fig. 1B, right), suggesting a slight growth attenuation of the recombinant rP18tri-G virus carrying the trisegmented genome. The efficiency of virus rescue from the trisegmented virus system is consistently high. At every rescue attempt, we obtained infectious viruses at 48 h posttransfection.

After purifying the viruses from single plaques, we conducted a growth curve analysis of the trisegmented rP18tri-G virus and the rP18 parental virus in BHK-21 cells at multiplicities of infection (MOIs) of 0.01 and 0.5. The rP18tri-G virus grew to lower levels (by ~1 to 1.5 log units) than the parental rP18 virus at both MOIs but could still reach a titer of 10^6 PFU/ml in BHK-21 cell cultures (Fig. 1C). In order to determine the stability of the rP18tri-G virus *in vitro*, we continuously passaged the rP18tri-G virus in BHK-21 cells; we conducted plaque assays at different passages and examined GFP expression for each of the plaques. At all passages tested (up to 23 passages), all plaques consistently expressed high levels of GFP, suggesting that the GFP-encoding S2 segment was stably maintained in the infectious viral particles even after extensive passages in cell culture. Taken together, these findings show that trisegmented rPICV can be efficiently rescued from plasmid-transfected cells and can grow to high titers *in vitro*.

We investigated the potential degree of virulence of the trisegmented rPICV in the established guinea pig model (23, 29). Guinea pigs were either mock infected with PBS or infected with 1×10^4 PFU of rP18tri-G or rP18 through the intraperitoneal route (*n*, 7 per group). As expected, all animals infected with the rP18 parental virus developed early-onset, prolonged fever, lost significant body weight, and reached terminal points by day 13 (Fig. 1D). In contrast, all rP18tri-G-infected animals survived the infection and showed a kinetics of body weight increase similar to that of the PBS group (Fig. 1D). Only a few of the rP18tri-G-infected animals experienced a brief 1-day fever (temperature, >39.5°C) (Fig. 1D). Therefore, the trisegmented rPICV is highly attenuated *in vivo*.

Generation of rP18tri vectors expressing GFP and influenza virus antigens. To establish the proof of concept for using rP18tri as a vaccine vector, we cloned the HA or NP gene of the influenza virus A/PR8/H1N1 strain into the P18 S1 plasmid and used it, together with the P18 L and S2-GFP plasmids, to generate rP18tri-G/H (encoding influenza virus HA) or rP18tri-G/P (encoding influenza virus NP), respectively (Fig. 2A). Upon infection of Vero cells, these viruses, as well as the control virus rP18tri-G, formed GFP-expressing foci that grew in size over the time course of infection (Fig. 2B). Both the rP18tri-G/H and rP18tri-G/P viruses showed growth kinetics similar to that of the rP18tri-G virus in BHK-21 cells (Fig. 2C), suggesting that the addition of the 1.7-kb HA gene or the 1.5-kb NP gene did not affect the replication capacity of the trisegmented PICV. To determine whether the influenza virus antigens were expressed upon viral infection, we infected Vero cells with either the rP18tri-G/H or the rP18tri-G/P virus at an MOI of 1 and, at 24 hpi, conducted an immunofluorescence assay (IFA) with an anti-HA or anti-NP antibody. Strong GFP expression was detected in cells infected by these viruses. HA or NP expression was detected in cells infected with rP18tri-G/H or rP18tri-G/P, respectively, but not in cells infected with rP18tri-G (Fig. 2D). We examined the stability of antigen expression after passaging rP18tri-G/H and rP18tri-G/P in cell culture 6

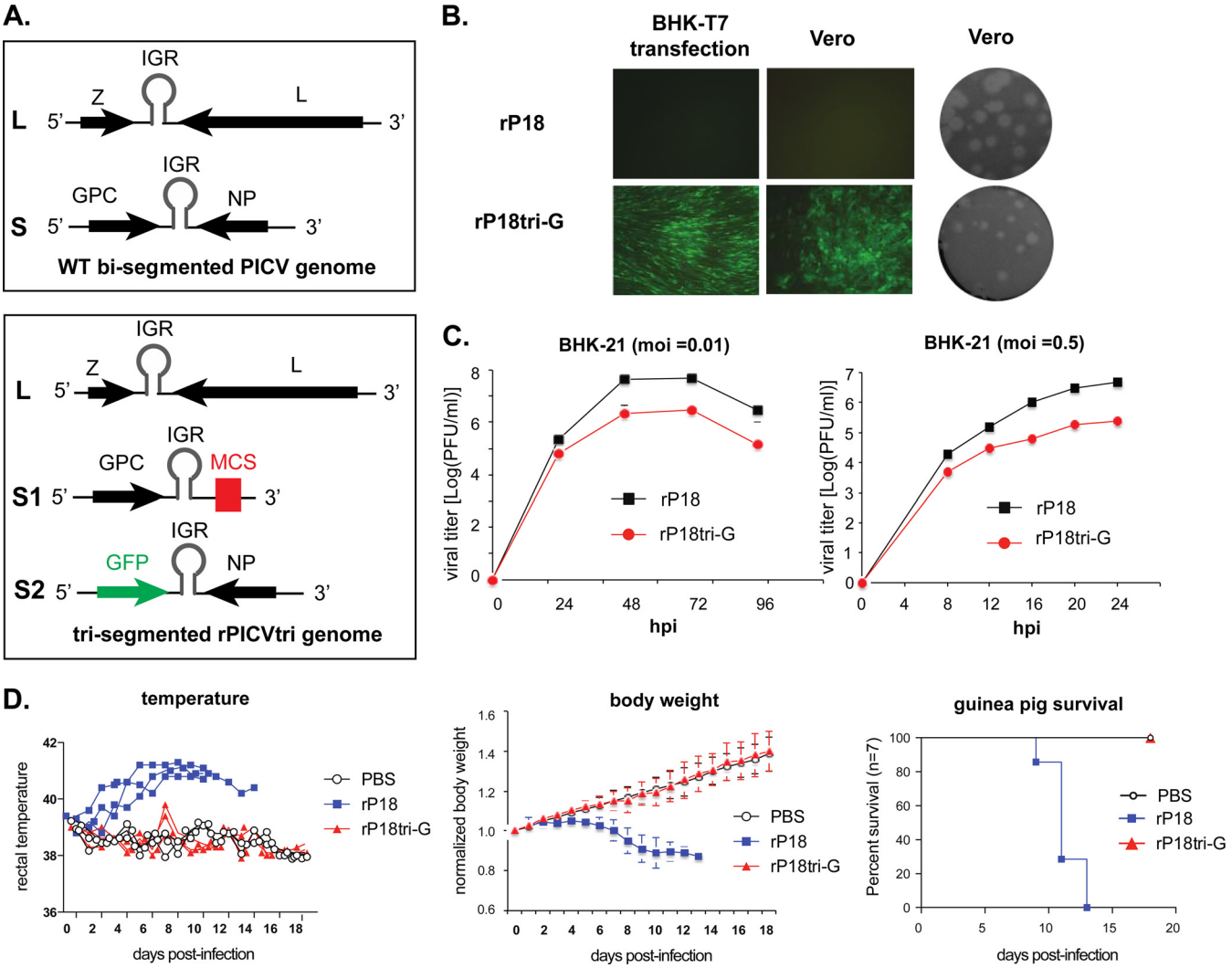

FIG 1 Development of a reverse genetics system to generate replication-competent trisegmented PICV (strain P18) expressing eGFP. (A) Schematic diagrams of the wild-type (WT) PICV genome with two genomic RNA segments (L and S) (top) and of the trisegmented rPICV genome (L, S1, and S2) encoding the eGFP reporter gene (bottom). IGR, intergenic region; MCS, multiple cloning sites. (B) Rescue of viable rP18tri-G virus from plasmid-transfected BSRT7-5 cells. BSRT7-5 cells were transfected with two plasmids, the L and S plasmids (for the rescue of rP18), or three plasmids, the L, S1, and S2 plasmids (for the rescue of rP18tri-G). Supernatants were collected from the transfected BSRT7-5 cells and were used to infect Vero cells. (Left) eGFP expression was observed in the transfected BSRT7-5 cells as well as in the infected Vero cells. (Right) Plaque assays of the rescued rP18 and rP18tri-G viruses were conducted on Vero cells. (C) Analysis of growth kinetics of the rP18 and rP18tri-G viruses in BHK-21 cells at MOIs of 0.01 and 0.5. The experiment was carried out twice in triplicate. (D) Comparison of degrees of virulence in guinea pigs infected with rP18 or rP18tri-G. Guinea pigs were either mock infected (PBS) or infected i.p. with 1×10^4 PFU of rP18 or rP18tri-G. (Left) Rectal temperatures; (center) normalized body weights; (right) survival curves.

times, and we could still detect HA and NP expression in Vero and BHK-21 cells infected with the respective viruses.

The rP18tri-G/H vaccine vector induces protective immunity against lethal influenza virus challenge in mice. We then used an established lethal influenza infection model to determine whether the rP18tri-G/H virus could induce protective immunity in mice (30). C57BL/6 mice were immunized with either the control vector rP18tri-G or rP18tri-G/H and were boosted once or twice with the same vectors at a 14-day interval. In the first trial, mice ($n = 3$) were given (i.p.) three doses each at 1×10^5 PFU. In the second trial, mice ($n = 3$) were given (i.p.) two doses each at 1×10^5 PFU. In the third trial, mice ($n = 5$) were given (i.m.) two doses each at 1×10^4 PFU. In the fourth trial, mice ($n = 3$) were given three doses each at 1×10^4 PFU via the i.m., i.m., and i.p. routes, respectively. At 14 days after the last vaccination dose, mice were challenged with 10 MLD_{50} of the mouse-adapted A/PR8 influenza virus. All mice vaccinated with rP18tri-G ($n = 14$) succumbed to the infection by 6 dpi, while all mice vaccinated with rP18tri-G/H ($n = 14$) were completely protected (Fig. 3A). The rP18tri-G/H-vaccinated mice did not show any disease phenotypes and maintained their body weights at levels similar to those of mock-infected mice, in sharp contrast to control vector-immunized mice, which rapidly lost body weight and reached terminal points upon influenza virus challenge (Fig. 3B). We also quantified viral loads in the lungs of some rP18tri-G-infected animals at day 6 postchallenge (6 dpi); these showed very high viral titers, ranging from 10^5 to 10^6 PFU/g, in contrast to viral loads for rP18tri-G/H-immunized mice, which were low or below the detection threshold (Fig. 3C).

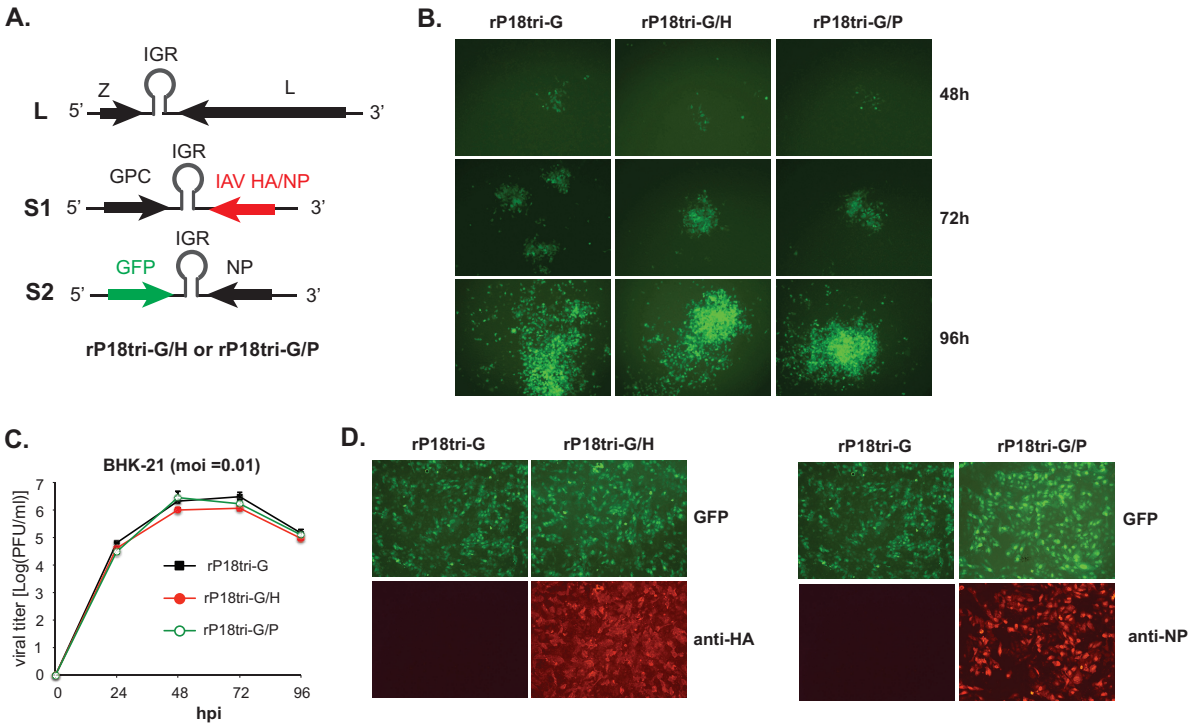

FIG 2 Generation of rP18tri vectors expressing eGFP together with an influenza A virus antigen. (A) Genomic organization of the rP18tri vector expressing eGFP together with influenza virus A/PR8 HA (rP18tri-G/H) or NP (rP18tri-G/P). IAV, influenza A virus; IGR, intergenic region. (B) The rP18tri-based vaccine vectors rP18tri-G, rP18tri-G/H, and rP18tri-G/P are replication competent. eGFP expression in the plasmid-transfected BSRT7-5 cells was detected under a fluorescence microscope at different times posttransfection. (C) Analysis of the viral growth kinetics of rP18tri-G, rP18tri-G/H, and rP18tri-G/P in BHK-21 cells at an MOI of 0.01. The experiment was carried out twice in triplicate. (D) Expression of eGFP (top) and influenza A virus HA or NP (bottom) in rP18tri vector-infected cells. Vero cells were infected (MOI, 1) with rP18tri-G, rP18tri-G/H, or rP18tri-G/P. At 24 hpi, eGFP expression was observed under a fluorescence microscope, while influenza HA or NP expression was detected by IFA using an anti-HA or anti-NP antibody.

To evaluate the sustaining effect of protection, we immunized mice with two doses of either rP18tri-G or rP18tri-G/H through the i.m. route at an interval of 3 weeks and then challenged these mice at 30, 60, and 120 days after the vaccination with a lethal dose of the mouse-adapted A/PR8 influenza virus. All of the rP18tri-G/H-immunized mice (n, $\geq$5 for each group) were completely protected from the lethal viral challenge, whereas the control vector group reached 100% mortality by day 7 (Fig. 3D). The vaccine-induced protective immunity was also supported by the histopathological data for mouse lungs 6 days after a lethal influenza virus challenge. We observed significant pathological changes, including airway obstruction and inflammatory cell infiltration, in the lungs of rP18tri-G vector-immunized mice, but not in those of rP18tri-G/H-vaccinated mice (Fig. 3E). We used immunohistochemical (IHC) staining with an anti-NP antibody to detect influenza virus in the lungs 6 days after challenge. Abundant viral antigens were present in the airway epithelial cells of the lungs from control vector-immunized mice, but no viral antigen was detected in the rP18tri-G/H-vaccinated mice (Fig. 3F). In contrast to the intact lung epithelium in the vaccinated mice, significant epithelial cell death and airway damage were observed in the control vector-immunized mice. Taken together, these data strongly suggest that the rP18tri-G/H viral vector can induce protective immunity against influenza virus infection in mice.

To test whether a single dose of rP18tri-G/H might still be able to provide protection, we immunized mice once with the rP18tri-G/H virus at 10^3, 10^4, or 10^5 PFU through the i.p. route, and 14 days later, we challenged them with a lethal dose of the mouse-adapted A/PR8 influenza virus. All mice (n, 3 for each group) survived the lethal challenge without showing any significant body weight loss (Fig. 3G), demonstrating that even a single low dose of rP18tri-G/H (10^3 PFU) can protect mice from lethal influenza virus infection. As expected, mice immunized with the control rP18tri-G virus at 10^5 PFU succumbed to virus infection, as evidenced by their dramatic body weight loss (Fig. 3G).

The rP18tri-G/H vaccine vector induces high neutralizing antibody titers. We next evaluated the levels of rP18tri-G/H-induced neutralizing antibodies by using the well-established hemagglutination inhibition (HAI) assay. For all the C57BL/6 mice immunized with the control vector rP18tri-G, HAI titers were below the detection limit (data not shown). A single vaccination dose of the rP18tri-G/H virus at 1×10^5 PFU, given by the i.m., i.n., or i.p. route, induced high HAI titers, ranging from 40 to 160, levels comparable to those induced by the formalin-inactivated influenza A/PR8 virus (Fig. 4A). There was no significant difference in HAI titers among the different inoculation routes. Furthermore, a single inoculation of rP18tri-G/H at different dosages—1×10^3, 1×10^4, or 1×10^5 PFU—induced comparable levels of HAI titers (Fig. 4B), a result that correlates with the protective immunity elicited by these dosages (Fig. 3G). In addition to C57BL/6 mice, we showed that rP18tri-G/H could also induce high HAI titers in BALB/c mice and that the HAI titers increased after a second inoculation (boost) with the same vaccine vector (Fig. 4C). Similarly, guinea pigs immunized once with rP18tri-

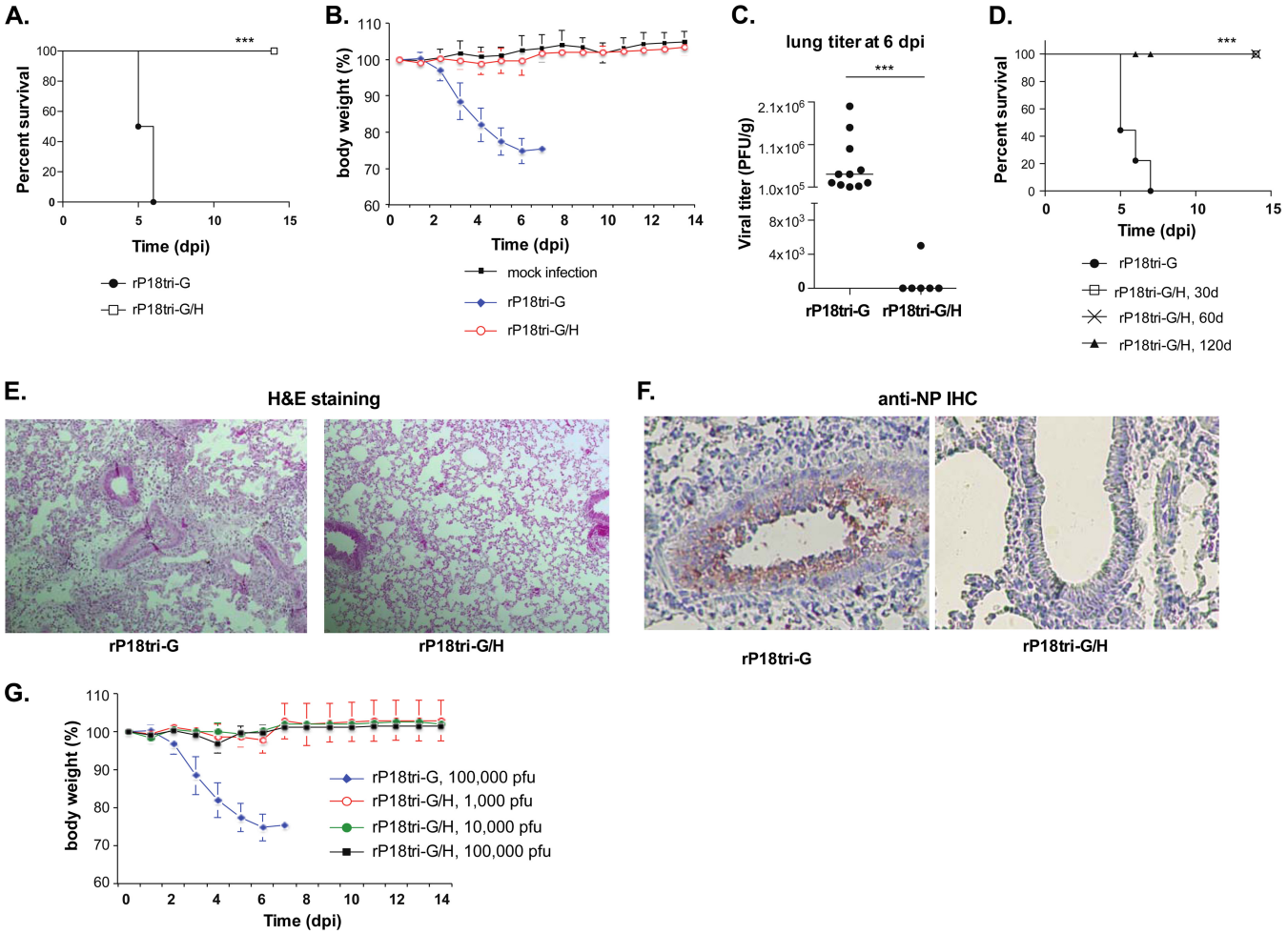

FIG 3 The rP18tri-G/H vector induces protective immunity against lethal influenza virus challenge in mice. (A and B) The rP18tri-G/H vector induces protective immunity in mice. A group of C57BL/6 mice ($n \geq 14$) were given either rP18tri-G or rP18tri-G/H at 1×10^5 PFU and were boosted once or twice with the same vaccine vector. Fourteen days after vaccination, mice were challenged i.n. with 10 MLD_{50} of the mouse-adapted influenza A/PR8 virus. Survival curves (A) and average body weights (B) are shown. (C) rP18tri-G/H-immunized mice can clear virus upon challenge. Influenza virus titers in the lungs at 6 dpi after a lethal influenza A/PR8 virus challenge were measured by plaque assays. (D) The rP18tri-G/H vector can induce sustained protective immunity. A group of C57BL/6 mice (n, ≥ 5) were given either the rP18tri-G or the rP18tri-G/H vector and were challenged with 10 MLD_{50} of influenza A/PR8 virus at 30, 60, and 120 days (d) after vaccination. Survival curves are shown. (E) H&E staining for comparison of lung histopathology in control and vaccinated mice after a lethal influenza A/PR8 virus challenge administered 60 days after vaccination. (F) IHC staining with an anti-NP antibody for comparison of viral antigens in control and vaccinated mice after a lethal influenza A/PR8 virus challenge administered 60 days after vaccination. (G) A single low dose of rP18tri-G/H is sufficient to induce complete protection. A group of C57BL/6 mice ($n = 3$) were immunized once with rP18tri-G or rP18tri-G/H at different doses (10^3, 10^4, and 10^5 PFU) and were challenged with 10 MLD_{50} of influenza A/PR8 virus. Average body weights of mice are shown. Statistical analyses of the survival curves were performed using the log rank (Mantel-Cox) χ^2 test in GraphPad Prism software, version 5. Statistical analysis of lung viral titers was conducted with the Student t test. ***, $P < 0.001$.

G/H (i.p.) produced high HAI titers (30 to 80) at 14 days after inoculation and even higher HAI titers (320 to 640) at 28 days (Fig. 4D). Taken together, our data suggest that the rP18tri-G/H vaccine vector can induce high levels of neutralizing antibodies in mice as well as in guinea pigs.

The rP18tri-G/P vaccine vector induces strong CTL responses in mice. We next assessed the T cell responses by using an established NP tetramer analysis based on its T cell epitope ASNENMETM(366-374). Splenic cells and/or peripheral blood mononuclear cells (PBMCs) were collected from mice 7 days after vaccination with either the control rP18tri-G virus or the rP18tri-G/P virus via different routes (i.m., i.p., i.n.) and were analyzed by FACS for H-2D^b-NP^{366}, CD3, CD8, and CD44. As shown in Fig. 5A, the CD3$^+$ CD8$^+$ cell population was gated, and the percentage of NP^{366}-tetramer-positive CD44^{high} cells in the population was determined. Compared to the vector control (rP18tri-G-immunized) group of mice, which showed a background level of NP-tetramer-positive CD8$^+$ CD44^{high} cells (0.14%), the rP18tri-G/P-immunized mice had distinctly higher levels of virus-specific CD8$^+$ CD44^{high} cells, ranging from 1.73 to 2.6%. We next quantified the T cell responses in groups of mice immunized with either the vector control (rP18tri-G) or rP18tri-G/P via the i.p. or i.m. route after either a single dose (prime) or a second dose (prime and boost). As expected, the vector control (rP18tri-G)-immunized mice produced background levels of NP-tetramer-positive CD8$^+$ CD44^{high} cells after either the prime only or the prime-and-boost regimen (Fig. 5B). In contrast, a single inoculation of rP18tri-G/P via either the i.p. or the i.m. route led to increases in

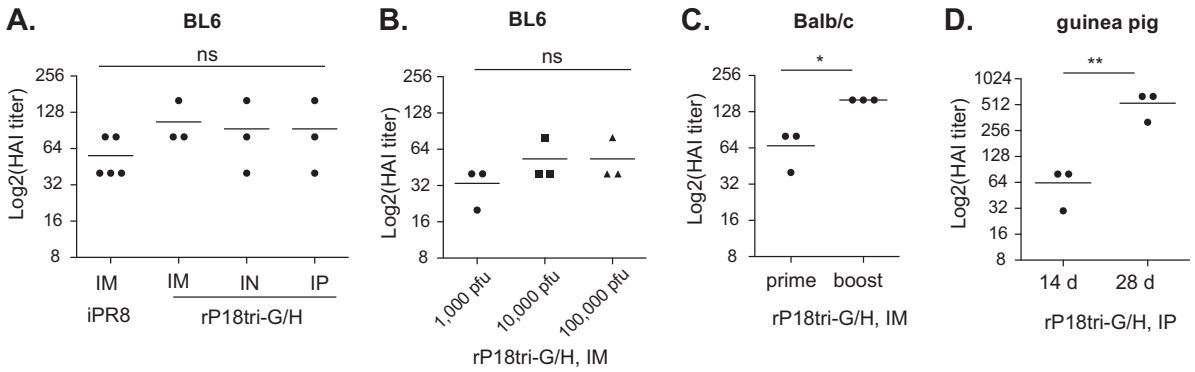

FIG 4 The rP18tri-G/H vector induces high neutralizing antibody titers. (A) HAI titers of C57BL/6 mice immunized i.m. with the formalin-inactivated influenza A/PR8 virus (iPR8) or with rP18tri-G/H given via the i.m., i.n., or i.p. route. (B) HAI titers of C57BL/6 mice immunized i.m. with rP18tri-G/H at different doses. (C) HAI titers of BALB/c mice immunized i.m. with rP18tri-G/H, determined 14 days after priming and after a boost vaccination. (D) HAI titers of guinea pigs at 14 and 28 days after a single i.p. administration of rP18tri-G/H. Statistical analyses were conducted using one-way analysis of variance in GraphPad Prism software, version 5. **, $P < 0.01$; *, $P < 0.05$; ns, not statistically significant.

the levels of virus-specific CD8 and CD44 cells to 1 to 4%, clearly above the background levels seen in the vector control group, even though statistical analysis showed a significant difference only between the i.m. and the control group (Fig. 5B, left). Interestingly, the virus-specific $CD8^+$ and $CD44^+$ T cell levels increased significantly after a boost dose of the rP18tri-G/P virus via the i.p. or i.m. route (Fig. 5B, right). No statistically significant difference in the level of T cell response was observed between the i.m. and i.p. routes after priming or after a prime-and-boost regimen. These data suggest that the rP18tri vector can induce virus-specific cytotoxic and memory-effector T cells.

The rP18tri-based vaccine vectors induce strong humoral and cellular immunity after repeated boosting. A perceived weakness of a live viral vector is the possibility that it may induce robust anti-vector immunity, which impairs the immune responses induced by the same vector and excludes its usage in a prime-boost vaccination strategy. We noticed that our rP18tri virus vectors appeared to induce even higher levels of neutralizing

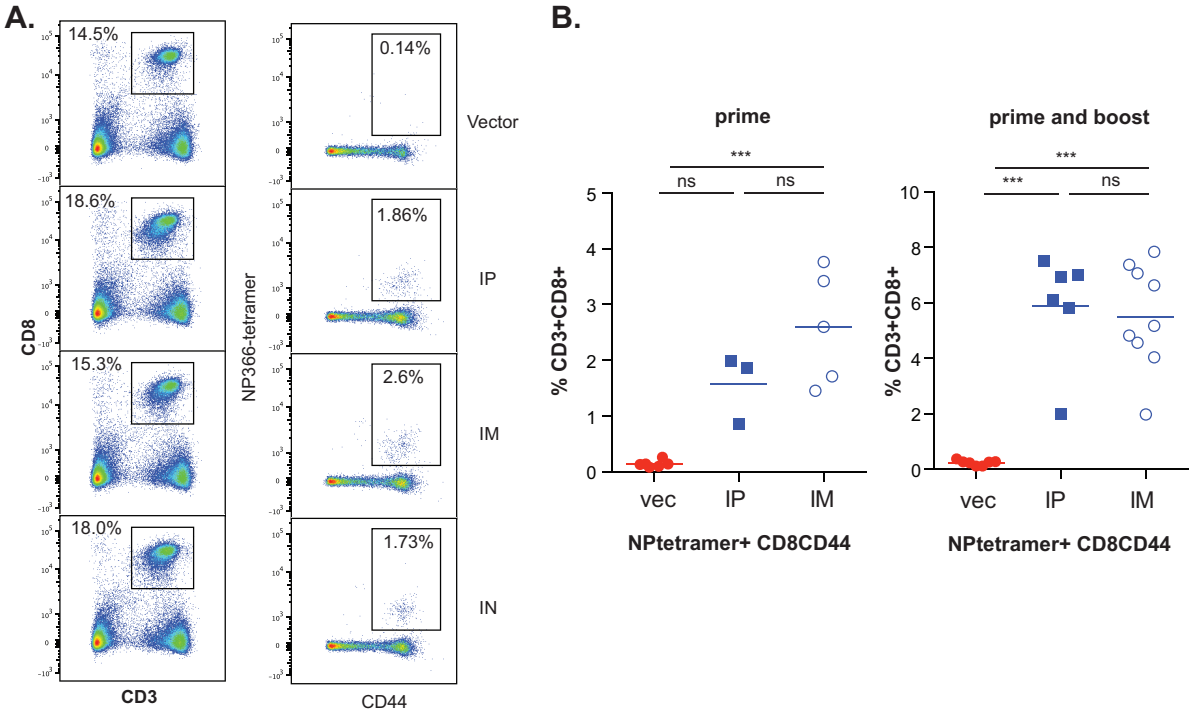

FIG 5 The rP18tri-G/P vector induces strong CTL responses in mice. (A) Influenza virus NP tetramer analysis. C57BL/6 mice were given rP18tri-G (control vector) or rP18tri-G/P via various routes (i.p., i.m., and i.n.). PBMCs were collected 7 days later for NP tetramer analysis as described in Materials and Methods. Results of a representative flow cytometric analysis are shown. (B) Vaccine-specific CTL responses after a prime (left) and a booster vaccination (right). vec, control vector. The level of NP tetramer-positive $CD8^+$ $CD44^{high}$ cells is shown as a percentage of the $CD3^+$ $CD8^+$ T cell population. Statistical analysis was conducted using one-way analysis of variance in GraphPad Prism software, version 5. ***, $P < 0.001$; ns, not statistically significant.

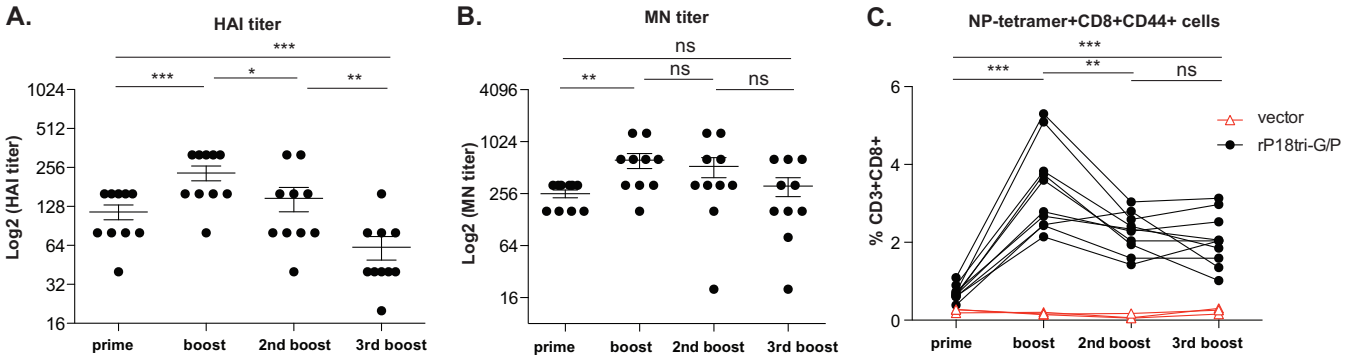

FIG 6 Quantification of vaccine-specific neutralizing antibodies and CTL responses after repeated administrations of the rP18tri vaccine vectors. C57BL/6 mice were given either the rP18tri-G control vector or a combination of rP18tri-G/H and rP18tri-G/P in a prime-and-repeated boost-vaccination strategy. (A and B) Sera were collected at 14 days after each administration and were analyzed by an HAI assay (A) and an MN assay (B) to evaluate the levels of vaccine-specific neutralizing antibodies. (C) PBMCs were collected at 7 days after each administration and were subjected to NP tetramer analysis as described in Materials and Methods. The level of NP tetramer-positive $CD8^+$ $CD44^{high}$ cells is shown as a percentage of the $CD3^+$ $CD8^+$ T cell population. Statistical analysis was conducted using the paired *t* test in GraphPad Prism software, version 5. ***, $P < 0.001$; **, $P < 0.01$; *, $P < 0.05$; ns, not statistically significant.

antibodies and T cell responses after a booster dose (Fig. 4C and 5B). To systematically monitor immune responses after repeated vaccination of the animals with the rP18tri vaccine vectors, we inoculated 10 mice via the i.m. route with a mixture of rP18tri-G/H and rP18tri-G/P, each at 1×10^4 PFU, and boosted three more times with the same mixture of viruses, with 21 days between inoculations. As vector controls, three mice were given rP18tri-G each time. PBMCs and blood were collected at 7 and 14 days after each administration and were used for analysis of T cell responses and levels of neutralization antibodies, respectively. Mice in the vector control group did not show HAI titers above the background level (<10), whereas all 10 mice in the rP18tri-G/H group had HAI titers above 40 after priming, and these titers increased significantly upon a booster vaccination (Fig. 6A). HAI titers decreased slightly after the second booster and further after the third but were still above 40 in all but one mouse (with an HAI titer of 20) (Fig. 6A).

We also evaluated the levels of influenza virus-specific neutralization antibodies by using the established microneutralization (MN) assay (31). As with HAI titers, all the rP18tri-G vector control-immunized mice had MN titers below the detection threshold, whereas the rP18tri-G/H-immunized mice had high MN titers after priming. MN titers increased further upon the first boost, remained high after the second, and decreased slightly after the third (Fig. 6B). Statistical analysis showed a significant difference in MN titers between the prime and prime-boost groups, but not between other groups. Taken together, our HAI and MN data showed that the levels of neutralizing antibodies induced by the rP18tri-G/H vectors were significantly upregulated upon a booster vaccination and remained at high levels even after the administration of four doses of the same vector. In a similar pattern, the level of NP tetramer-positive $CD8^+$ $CD44^{high}$ cells (Fig. 6C) increased significantly upon a booster dose and decreased slightly after the second and third boosts but still remained significantly higher than after priming. Taking these findings together, we show that both humoral and cellular vaccine immunity induced by the rP18tri vector are further strengthened by a booster vaccination and remain at relatively high levels even after repeated administration.

DISCUSSION

We report here the development of a PICV-based (rP18tri) live viral vaccine vector that can elicit strong immunity in mice. Using influenza virus HA or NP as a model antigen, we show that the rP18tri-based vector can induce high levels of HA-specific neutralizing antibodies and strong NP-specific CTL responses. Interestingly, the vaccine-induced immunity appears to increase upon a booster vaccination and remains at a relatively high level even after multiple repeated administrations. We therefore believe that this rP18tri vector can be developed into a useful vaccine platform against various human diseases, particularly when strong cellular immunity and a prime-boost vaccination strategy are desired.

Vaccines are the most cost-effective measure for the control of infectious diseases. Many successful vaccines are based on live-attenuated pathogens and usually confer strong and long-lasting immunity (32, 33). Compared to inactivated vaccines, live viral vaccines are known to induce strong cellular immunity, which is important for combating various human diseases ranging from microbial infections to cancers. Each of the currently available live viral vectors has its pros and cons, and none has proven to be universally suitable for every pathogen (13, 34). An ideal viral vector must be safe, induce strong and durable cellular and humoral immune responses, have no preexisting immunity, and, ideally, not lose potency upon repeated application.

A trisegmented LCMV system was first developed by Emonet et al. (15) and has offered an opportunity for gene delivery (16). Recently, the trisegmented vaccine platforms based on LCMV and the Junin virus (JUNV) vaccine strain Candid#1 have been developed and propagated in the Food and Drug Administration (FDA)-approved Vero cell line (17). The PICV-based vector system described in this work has several advantages as a potential vaccine platform. In contrast to LCMV, which has a 2% to 5% seroprevalence in the general human population, PICV has a very low seroprevalence as suggested by serological evidence, even in the local human population in Columbia, where PICV was originally isolated from rice rats (19). Therefore, there is little to no preexisting immunity against PICV in the general human population. Unlike LCMV and JUNV, for which the Candid#1 vaccine strain has been developed, PICV is generally not known to cause

diseases in humans. Moreover, relative to the wild-type parental virus (PICV strain rP18), the trisegmented rP18tri vector is attenuated *in vitro* (Fig. 1C) and *in vivo* (Fig. 1D and E), possibly due to the necessity of packaging three, rather than two, viral genomic RNA segments into budding viral particles and to the increase in the size of the viral genome. We believe that this growth attenuation further improves the biosafety profile of the rP18tri vector.

Like other arenaviruses, PICV infects DCs and macrophages early in infection. Targeting these professional antigen-presenting cells (APCs) can enhance the presentation of antigens to the immune system and leads to an increase in the frequency and avidity of specific adaptive immunity. We show in this work that the rP18tri vector can induce complete protection in mice after a single low-dose immunization. Strong humoral and cellular immunity can be induced via different tested routes (i.m., i.p., and i.n.) and, surprisingly, is further increased significantly by a booster dose. High levels of vaccine-specific neutralizing antibodies and CTL responses can still be detected even after four inoculations of the same rP18tri vector, possibly due to the low level of PICV-specific neutralizing antibodies. Similar observations of low anti-vector immunity have been reported for a replication-defective LCMV vector (14) and a replication-competent vesicular stomatitis virus pseudotyped with the LCMV GPC (VSV-GP) (35). The lack of vector-neutralizing antibodies in VSV-GP-immunized mice is a feature attributed to LCMV GPC, since it has been shown that LCMV GPC, and not the vector, determines the kinetics of neutralizing antibody development (36). Our data with the rP18tri vector suggest that PICV GPC may have characteristics similar to those of the LCMV GPC in terms of being a poor inducer of neutralizing antibodies. Using a microneutralization assay, we could not detect any PICV-specific neutralizing antibodies in mice after a prime and boost with either rPICV or rP18tri-G in a preliminary study. In contrast to other live viral vectors in general, booster exposure of the rP18tri vector leads to further enhanced vaccine immunity at both the antibody and T cell levels, the mechanism of which remains to be characterized. Additional repeated administrations (third and fourth doses) reduce vaccine immunity from peak levels, possibly due to anti-vector immunity; however, it is worth noting that the antigen-specific T cell responses are still higher than those after priming, and the MN titers remain at the same level as those after priming. Further studies are required to mechanistically characterize the changes in the vaccine immune responses upon repeated applications of the rP18tri vector.

Despite the current vaccine program and existing antivirals, influenza viruses remain a global threat to human health due to their constantly evolving nature. Current seasonal flu vaccines have variable protection rates, require yearly updating, and are unavailable for early pandemic and zoonotic infections (37). Multiple strategies have been attempted to develop a universal flu vaccine that confers broad-spectrum protection against multiple influenza virus subtypes, including the development of cross-reactive antibodies against the conserved HA stalk region, the conserved eM2 epitope, and the conserved NP, as well as the induction of T cell responses (38–40). Several recent studies have suggested that broadly neutralizing antibodies can be generated by prime-and-boost vaccinations or sequential infections (41–47). In addition, since T cell epitopes (mostly within M1 and NP) are conserved between subtypes, elicitation of antigen-specific T cell responses is expected to confer broadly protective immunity. Our study suggests that this novel rP18tri vector can be used to develop cross-reactive immunity against influenza virus subtypes due to its ability to deliver multiple antigens, to elicit strong immune responses including robust cellular immunity, and to enhance vaccine immunity after a booster dose.

In summary, using the influenza virus HA and NP as model antigens, we have demonstrated the prowess and versatility of the trisegmented rP18tri vector at inducing effective vaccine immunity at both the humoral and T cell levels. More importantly, the unique feature of the trisegmented rP18tri vector—showing enhanced immune responses upon a booster dose—makes this vector ideal for use in a prime-and-boost vaccination strategy.

ACKNOWLEDGMENTS

We acknowledge the NIH Tetramer Core Facility (contract HHSN272201300006C) for the provision of the PE-labeled H-2D^b/influenza virus NP$_{366-374}$ tetramer. We thank K.-K. Conzelmann (Ludwig-Maximilians-Universität, Munich, Germany) for the BSRT7-5 cells.

This work was partly supported by NIH grants R21AI094133 and R01AI083409 (to Y.L.) and AI093580 (to H.L.).

FUNDING INFORMATION

HHS | NIH | National Institute of Allergy and Infectious Diseases (NIAID) provided funding to Yuying Liang under grant numbers R01AI083409 and R21AI094133. HHS | NIH | National Institute of Allergy and Infectious Diseases (NIAID) provided funding to Hinh Ly under grant number AI093580.

REFERENCES

1. **Buchmeier MJ, De La Torre JC, Peters CJ.** 2007. *Arenaviridae*: the viruses and their replication, p 1791–1827. *In* Knipe DM, Howley PM, Griffin DE, Lamb RA, Martin MA, Roizman B, Straus SE (ed), Fields virology, 5th ed. Lippincott Williams & Wilkins, Philadelphia, PA.
2. **Ng CT, Snell LM, Brooks DG, Oldstone MB.** 2013. Networking at the level of host immunity: immune cell interactions during persistent viral infections. Cell Host Microbe **13:**652–664. http://dx.doi.org/10.1016/j.chom.2013.05.014.
3. **Zhou X, Ramachandran S, Mann M, Popkin DL.** 2012. Role of lymphocytic choriomeningitis virus (LCMV) in understanding viral immunology: past, present and future. Viruses **4:**2650–2669. http://dx.doi.org/10.3390/v4112650.
4. **Fehling SK, Lennartz F, Strecker T.** 2012. Multifunctional nature of the arenavirus RING finger protein Z. Viruses **4:**2973–3011. http://dx.doi.org/10.3390/v4112973.
5. **Xing J, Ly H, Liang Y.** 2015. The Z proteins of pathogenic but not nonpathogenic arenaviruses inhibit RIG-I-like receptor-dependent interferon production. J Virol **89:**2944–2955. http://dx.doi.org/10.1128/JVI.03349-14.
6. **Salvato M, Shimomaye E, Oldstone MB.** 1989. The primary structure of the lymphocytic choriomeningitis virus L gene encodes a putative RNA polymerase. Virology **169:**377–384. http://dx.doi.org/10.1016/0042-6822(89)90163-3.
7. **Burri DJ, da Palma JR, Kunz S, Pasquato A.** 2012. Envelope glycoprotein of arenaviruses. Viruses **4:**2162–2181. http://dx.doi.org/10.3390/v4102162.
8. **McLay L, Ansari A, Liang Y, Ly H.** 2013. Targeting virulence mechanisms for the prevention and therapy of arenaviral hemorrhagic fever. Antiviral Res **97:**81–92. http://dx.doi.org/10.1016/j.antiviral.2012.12.003.
9. **Pinschewer DD, Perez M, de la Torre JC.** 2003. Role of the virus nucleoprotein in the regulation of lymphocytic choriomeningitis virus transcription and RNA replication. J Virol **77:**3882–3887. http://dx.doi.org/10.1128/JVI.77.6.3882-3887.2003.
10. **Lee KJ, Novella IS, Teng MN, Oldstone MB, de La Torre JC.** 2000. NP and L proteins of lymphocytic choriomeningitis virus (LCMV) are sufficient for efficient transcription and replication of LCMV genomic RNA analogs. J Virol **74:**3470–3477. http://dx.doi.org/10.1128/JVI.74.8.3470-3477.2000.
11. **Martínez-Sobrido L, Zuniga EI, Rosario D, Garcia-Sastre A, de la Torre**

JC. 2006. Inhibition of the type I interferon response by the nucleoprotein of the prototypic arenavirus lymphocytic choriomeningitis virus. J Virol **80:**9192–9199. http://dx.doi.org/10.1128/JVI.00555-06.
12. **Qi X, Lan S, Wang W, Schelde LM, Dong H, Wallat GD, Ly H, Liang Y, Dong C.** 2010. Cap binding and immune evasion revealed by Lassa nucleoprotein structure. Nature **468:**779–783. http://dx.doi.org/10.1038/nature09605.
13. **Huang Q, Shao J, Lan S, Zhou Y, Xing J, Dong C, Liang Y, Ly H.** 2015. *In vitro* and *in vivo* characterizations of the Pichinde viral NP exoribonuclease function. J Virol http://dx.doi.org/10.1128/JVI.00009-15.
14. **Flatz L, Hegazy AN, Bergthaler A, Verschoor A, Claus C, Fernandez M, Gattinoni L, Johnson S, Kreppel F, Kochanek S, Broek M, Radbruch A, Levy F, Lambert PH, Siegrist CA, Restifo NP, Lohning M, Ochsenbein AF, Nabel GJ, Pinschewer DD.** 2010. Development of replication-defective lymphocytic choriomeningitis virus vectors for the induction of potent $CD8^+$ T cell immunity. Nat Med **16:**339–345. http://dx.doi.org/10.1038/nm.2104.
15. **Emonet SF, Garidou L, McGavern DB, de la Torre JC.** 2009. Generation of recombinant lymphocytic choriomeningitis viruses with trisegmented genomes stably expressing two additional genes of interest. Proc Natl Acad Sci U S A **106:**3473–3478. http://dx.doi.org/10.1073/pnas.0900088106.
16. **Popkin DL, Teijaro JR, Lee AM, Lewicki H, Emonet S, de la Torre JC, Oldstone M.** 2011. Expanded potential for recombinant trisegmented lymphocytic choriomeningitis viruses: protein production, antibody production, and in vivo assessment of biological function of genes of interest. J Virol **85:**7928–7932. http://dx.doi.org/10.1128/JVI.00486-11.
17. **Ortiz-Riaño E, Cheng BY, de la Torre JC, Martinez-Sobrido L.** 2013. Arenavirus reverse genetics for vaccine development. J Gen Virol **94:**1175–1188. http://dx.doi.org/10.1099/vir.0.051102-0.
18. **McLay L, Liang Y, Ly H.** 2014. Comparative analysis of disease pathogenesis and molecular mechanisms of New World and Old World arenavirus infections. J Gen Virol **95:**1–15. http://dx.doi.org/10.1099/vir.0.057000-0.
19. **Trapido H, Sanmartin C.** 1971. Pichinde virus, a new virus of the Tacaribe group from Colombia. Am J Trop Med Hyg **20:**631–641.
20. **Centers for Disease Control and Prevention.** 6 May 2014, revision date. Lymphocytic choriomeningitis (LCM). Centers for Disease Control and Prevention, Atlanta, GA. http://www.cdc.gov/vhf/lcm/.
21. **Buchmeier M, Adam E, Rawls WE.** 1974. Serological evidence of infection by Pichinde virus among laboratory workers. Infect Immun **9:**821–823.
22. **Rosenthal KL, Steiner C, Rawls WE, Walker CM.** 1986. Studies concerning the relationship of Pichinde virus-induced natural killer cells and cytotoxic T lymphocytes. Med Microbiol Immunol **175:**133–136. http://dx.doi.org/10.1007/BF02122433.
23. **Lan S, McLay Schelde L, Wang J, Kumar N, Ly H, Liang Y.** 2009. Development of infectious clones for virulent and avirulent Pichinde viruses: a model virus to study arenavirus-induced hemorrhagic fevers. J Virol **83:**6357–6362. http://dx.doi.org/10.1128/JVI.00019-09.
24. **Liang Y, Lan S, Ly H.** 2009. Molecular determinants of Pichinde virus infection of guinea pigs—a small animal model system for arenaviral hemorrhagic fevers. Ann N Y Acad Sci **1171**(Suppl 1)**:**E65–E74. http://dx.doi.org/10.1111/j.1749-6632.2009.05051.x.
25. **Kumar N, Wang J, Lan S, Danzy S, McLay Schelde L, Seladi-Schulman J, Ly H, Liang Y.** 2012. Characterization of virulence-associated determinants in the envelope glycoprotein of Pichinde virus. Virology **433:**97–103. http://dx.doi.org/10.1016/j.virol.2012.07.009.
26. **Wang J, Danzy S, Kumar N, Ly H, Liang Y.** 2012. Biological roles and functional mechanisms of arenavirus Z protein in viral replication. J Virol **86:**9794–9801. http://dx.doi.org/10.1128/JVI.00385-12.
27. **Jiang X, Huang Q, Wang W, Dong H, Ly H, Liang Y, Dong C.** 2013. Structures of arenaviral nucleoproteins with triphosphate dsRNA reveal a unique mechanism of immune suppression. J Biol Chem **288:**16949–16959. http://dx.doi.org/10.1074/jbc.M112.420521.
28. **McLay L, Lan S, Ansari A, Liang Y, Ly H.** 2013. Identification of virulence determinants within the L genomic segment of the Pichinde arenavirus. J Virol **87:**6635–6643. http://dx.doi.org/10.1128/JVI.00044-13.
29. **Aronson JF, Herzog NK, Jerrells TR.** 1994. Pathological and virological features of arenavirus disease in guinea pigs. Comparison of two Pichinde virus strains. Am J Pathol **145:**228–235.
30. **Matsuoka Y, Lamirande EW, Subbarao K.** 2009. The mouse model for influenza. Curr Protoc Microbiol Chapter 15:Unit 15G.3. http://dx.doi.org/10.1002/9780471729259.mc15g03s13.
31. **WHO Global Influenza Surveillance Network.** 2011. Manual for the laboratory diagnosis and virological surveillance of influenza. World Health Organization, Geneva, Switzerland.
32. **Robert-Guroff M.** 2007. Replicating and non-replicating viral vectors for vaccine development. Curr Opin Biotechnol **18:**546–556. http://dx.doi.org/10.1016/j.copbio.2007.10.010.
33. **Rollier CS, Reyes-Sandoval A, Cottingham MG, Ewer K, Hill AV.** 2011. Viral vectors as vaccine platforms: deployment in sight. Curr Opin Immunol **23:**377–382. http://dx.doi.org/10.1016/j.coi.2011.03.006.
34. **Small JC, Ertl HC.** 2011. Viruses—from pathogens to vaccine carriers. Curr Opin Virol **1:**241–245. http://dx.doi.org/10.1016/j.coviro.2011.07.009.
35. **Tober R, Banki Z, Egerer L, Muik A, Behmuller S, Kreppel F, Greczmiel U, Oxenius A, von Laer D, Kimpel J.** 2014. VSV-GP: a potent viral vaccine vector that boosts the immune response upon repeated applications. J Virol **88:**4897–4907. http://dx.doi.org/10.1128/JVI.03276-13.
36. **Pinschewer DD, Perez M, Jeetendra E, Bachi T, Horvath E, Hengartner H, Whitt MA, de la Torre JC, Zinkernagel RM.** 2004. Kinetics of protective antibodies are determined by the viral surface antigen. J Clin Invest **114:**988–993. http://dx.doi.org/10.1172/JCI200422374.
37. **Fiore AE, Bridges CB, Cox NJ.** 2009. Seasonal influenza vaccines. Curr Top Microbiol Immunol **333:**43–82. http://dx.doi.org/10.1007/978-3-540-92165-3_3.
38. **Shaw A.** 2012. New technologies for new influenza vaccines. Vaccine **30:**4927–4933. http://dx.doi.org/10.1016/j.vaccine.2012.04.095.
39. **Jang YH, Seong BL.** 2014. Options and obstacles for designing a universal influenza vaccine. Viruses **6:**3159–3180. http://dx.doi.org/10.3390/v6083159.
40. **Pica N, Palese P.** 2013. Toward a universal influenza virus vaccine: prospects and challenges. Annu Rev Med **64:**189–202. http://dx.doi.org/10.1146/annurev-med-120611-145115.
41. **Wei CJ, Boyington JC, McTamney PM, Kong WP, Pearce MB, Xu L, Andersen H, Rao S, Tumpey TM, Yang ZY, Nabel GJ.** 2010. Induction of broadly neutralizing H1N1 influenza antibodies by vaccination. Science **329:**1060–1064. http://dx.doi.org/10.1126/science.1192517.
42. **Wei CJ, Yassine HM, McTamney PM, Gall JG, Whittle JR, Boyington JC, Nabel GJ.** 2012. Elicitation of broadly neutralizing influenza antibodies in animals with previous influenza exposure. Sci Transl Med **4:**147ra114. http://dx.doi.org/10.1126/scitranslmed.3004273.
43. **Miller MS, Gardner TJ, Krammer F, Aguado LC, Tortorella D, Basler CF, Palese P.** 2013. Neutralizing antibodies against previously encountered influenza virus strains increase over time: a longitudinal analysis. Sci Transl Med **5:**198ra107. http://dx.doi.org/10.1126/scitranslmed.3006637.
44. **Wrammert J, Koutsonanos D, Li GM, Edupuganti S, Sui J, Morrissey M, McCausland M, Skountzou I, Hornig M, Lipkin WI, Mehta A, Razavi B, Del Rio C, Zheng NY, Lee JH, Huang M, Ali Z, Kaur K, Andrews S, Amara RR, Wang Y, Das SR, O'Donnell CD, Yewdell JW, Subbarao K, Marasco WA, Mulligan MJ, Compans R, Ahmed R, Wilson PC.** 2011. Broadly cross-reactive antibodies dominate the human B cell response against 2009 pandemic H1N1 influenza virus infection. J Exp Med **208:**181–193. http://dx.doi.org/10.1084/jem.20101352.
45. **Krammer F, Pica N, Hai R, Tan GS, Palese P.** 2012. Hemagglutinin stalk-reactive antibodies are boosted following sequential infection with seasonal and pandemic H1N1 influenza virus in mice. J Virol **86:**10302–10307. http://dx.doi.org/10.1128/JVI.01336-12.
46. **Miller MS, Tsibane T, Krammer F, Hai R, Rahmat S, Basler CF, Palese P.** 2013. 1976 and 2009 H1N1 influenza virus vaccines boost anti-hemagglutinin stalk antibodies in humans. J Infect Dis **207:**98–105. http://dx.doi.org/10.1093/infdis/jis652.
47. **Margine I, Hai R, Albrecht RA, Obermoser G, Harrod AC, Banchereau J, Palucka K, Garcia-Sastre A, Palese P, Treanor JJ, Krammer F.** 2013. H3N2 influenza virus infection induces broadly reactive hemagglutinin stalk antibodies in humans and mice. J Virol **87:**4728–4737. http://dx.doi.org/10.1128/JVI.03509-12.